Generation and Phenotype of a Transgenic Knockout Mouse Lacking the Mercurial-insensitive Water Channel Aquaporin-4

Tonghui Ma, Baoxue Yang, Annemarie Gillespie, Elaine J. Carlson, Charles J. Epstein, and A.S. Verkman
Department of Medicine, Department of Physiology, and Department of Pediatrics, Cardiovascular Research Institute, University of California, San Francisco, California 94143-0521

Abstract

Aquaporin-4 (AQP4) is a mercurial-insensitive, water-selective channel that is expressed in astroglia and basolateral plasma membranes of epithelia in the kidney collecting duct, airways, stomach, and colon. A targeting vector for homologous recombination was constructed using a 7-kb SacI AQP4 genomic fragment in which part of the exon 1 coding sequence was deleted. Analysis of 164 live births from AQP4[+/−] matings showed 41 [+/+], 83 [+/−], and 40 [−/−] genotypes. The [−/−] mice expressed small amounts of a truncated AQP4 transcript and lacked detectable AQP4 protein by immunoblot analysis and immunocytochemistry. Water permeability in an AQP4-enriched brain vesicle fraction in [+/+] mice was high and mercurial insensitive, and was decreased by 14-fold in [−/−] mice. AQP4 deletion did not affect growth or tissue morphology at the light microscopic level. Northern blot analysis showed that tissue-specific expression of AQPs 1, 2, 3, and 5 was not affected by AQP4 deletion. Maximum urine osmolality after a 36-h water deprivation was (in mosM, $n = 15$) [+/+] 3,342±209, [+/−] 3,225±167, and [−/−] 2,616±229 ($P < 0.025$), whereas urine osmolalities before water deprivation did not differ among the genotypes. Rotorod analysis of 35–38-d-old mice revealed no differences in neuromuscular function (performance time in s, $n = 8$): [+/+] 297±25, [+/−] 322±28, [−/−] 288±37. These results indicate that AQP4 deletion in CD1 mice has little or no effect on development, survival, growth, and neuromuscular function, but produces a small defect in urinary concentrating ability consistent with its expression in the medullary collecting duct. (*J. Clin. Invest.* 1997. 100:957–962.) Key words: water transport • aquaporin • AQP4 • mercurial-insensitive water channel • urinary concentration

Introduction

Several water transporting proteins (aquaporins, AQPs)[1] with homology to the major intrinsic protein of lens fiber (MIP, reference 1) have been identified in mammals. AQP1 (original name CHIP28, reference 2) is found in erythrocytes, the kidney proximal tubule, and various epithelia and endothelia. AQP2 (original name WCH-CD, reference 3) is the vasopressin-inducible water channel expressed in the kidney collecting duct. AQP3 (alternate name GLIP, glycerol transporting intrinsic protein) was cloned by several laboratories (4–6), and is expressed at the basolateral membrane of the kidney collecting duct and multiple epithelia (7). AQP4 (original name MIWC, mercurial-insensitive water channel, reference 8) is expressed strongly in the brain and colocalizes with AQP3 in several tissues (see below). AQP5 (9) is expressed in the lung, salivary gland, and eye. Functional studies indicate that the AQPs form water-selective channels, except for AQP3, which also transports glycerol and possibly other small polar solutes. Amino acid sequence analysis indicates several conserved sequences among the AQPs, but with overall amino acid identities of only 25–60%.

Although a considerable body of information exists on the genetics, tissue localization, structure, and function of mammalian AQPs, little is known about their role in normal physiology and disease. Whereas human subjects lacking AQP1 are phenotypically normal (10), mutations in AQP2 cause non–X-linked nephrogenic diabetes insipidus (11). No natural mutations or knockout models for AQPs 3, 4, and 5 have been identified, nor do selective or nontoxic inhibitors exist for any AQP.

The purpose of this study was to generate and characterize a transgenic null mouse lacking AQP4. AQP4 was initially cloned from rat lung (8). Subsequently, an isoform with an extended amino terminus was found in rat brain (12), and homologs from human (13) and mouse (14) were cloned. Immunocytochemistry showed rat AQP4 protein expression at the basolateral membrane of the kidney collecting duct, ependymal cells lining brain ventricles, astroglial cells in the brain and spinal cord, skeletal muscle sarcolemma, and epithelial cells in the stomach, trachea, airways, and colon (7, 15). AQP4 is unique among the mammalian AQPs in that (*a*) its water permeability is not inhibited by mercurials (because of absence of a cysteine residue at a critical location, reference 16), (*b*) its single-channel water permeability is three- to fourfold higher than that of the other water channels (17), and (*c*) it is spatially organized in cell membranes in square orthogonal arrays (18).

Address correspondence to Alan S. Verkman, M.D., Ph.D., 1246 Health Sciences East Tower, Cardiovascular Research Institute, University of California, San Francisco, San Francisco, CA 94143-0521. Phone: 415-476-8530; FAX: 415-665-3847; E-mail: verkman@itsa.ucsf.edu

Received for publication 20 March 1997 and accepted in revised form 12 June 1997.

J. Clin. Invest.

0021-9738/97/09/0957/06 $2.00
Volume 100, Number 5, September 1997, 957–962
http://www.jci.org

1. *Abbreviations used in this paper:* AQP, aquaporin; ES, embryonic stem; P_f, osmotic water permeability.

Based on tissue localization (7, 15) and functional data (19, 20), it was proposed that AQP4 plays a role in neuromuscular function, the urinary concentrating mechanism, airway hydration, and fecal dehydration. The AQP4 null mouse described here was used to test whether AQP4 is important for growth and development, whether AQP4 deletion is associated with tissue-specific upregulation of other AQPs, and whether AQP4 deletion is associated with defective renal or neuromuscular function.

Methods

Targeting vector construction and embryonic stem (ES) cell screening. Based on the genomic analysis of mouse AQP4 (14), an AQP4 replacement targeting vector was constructed using a 7-kb genomic SacI DNA fragment containing exons 1–3 and part of exon 4 (Fig. 1). Part of the exon 1 coding sequence (bp 298–381) into ~1 kb of intron 1 was replaced by a 1.8-kb PolIIneobpA cassette for positive selection. A 3-kb PGK-tk cassette was inserted at the 3′-end of the right arm for negative selection. The targeting vector was linearized at a unique NotI site downstream from the PGK-tk cassette and electroporated into CB1-4 ES cells as described previously (21). Transfected ES cells were selected with G418 (300 μg/ml) and FIAU (1-[2-deoxy, 2-fluoro B-D arabinofuranosyl]-5-iodouracil, 0.3 μM) for 7 d. Out of 287 doubly resistant colonies, five properly targeted clones were identified by PCR amplification of a 1.3-kb fragment using a sense primer specific for the *AQP4* gene (p_{AQP4}) (5′-TATATGTGTGTGCTTACATAATGAAATACG-3′) located upstream from the 5′-end of the construct, and an antisense primer specific for the neo cassette promoter (p_{neo}) (5′-CACCGCTGAATATGCATAAGGCA-3′). Homologous recombination was confirmed by Southern hybridization: 10 μg genomic DNAs was digested with EcoRI and resolved on a 7% agarose gel. The gel was alkaline-blotted to a positively charged Nylon plus membrane (Amersham Corp., Arlington Heights, IL) and hybridized for 1 h at 68°C in rapid hyb buffer (Amersham Corp.) with a ^{32}P-labeled 2.4-kb genomic fragment located downstream from the targeting vector and upstream from the EcoRI site (Fig. 1). The washed membranes were autoradiographed overnight at room temperature.

Generation of AQP4 knockout mice. ES cells were injected into PC 2.5 day 8 cell morula stage CD1 zygotes, cultured overnight to blastocysts, and transferred to pseudopregnant B6D2 females. Offspring were genotyped by PCR using primers: p_{AQP4}-sense, 5′-ACCATAAACTGGGGTGGCTCAG-3′ (corresponding to exon 1, bp 100–121); p_{AQP4}-antisense, 5′-TAGAGGATGCCGGCTCCAATGA-3′ (corresponding to the deleted part of exon 1, bp 325-314); p_{neo}, 5′-CACCGCTGAATATGCATAAGGCA-3′; and by Southern blot analysis as described above. Mice heterozygous for the AQP4 mutation were intercrossed to produce homozygous knockout mice.

Northern blot analysis. Total RNAs from the brain, kidney, and lung were isolated by homogenization in guanidinium thiocyanate followed by phenol-chloroform extraction. RNAs (10 μg/lane) were resolved on a formaldehyde-agarose denaturing gel and transferred to positively charged Nylon plus membrane (Amersham Corp.). The blotted membranes were hybridized with ^{32}P-labeled probes corresponding to each of the cDNA coding regions of AQPs 1–5 using the conditions for Southern blotting described above.

Immunoblot analysis. Tissues were homogenized in 250 mM sucrose, 10 mM Tris-HCl, pH 7.4, containing 1 μg/ml leupeptin, 1 μg/ml pepstatin A, and 4 μg/ml antipain. A membrane pellet was prepared by removal of nuclei and debris (3,000 *g* for 10 min) followed by centrifugation at 100,000 *g* for 60 min. Proteins were resolved on a 12% polyacrylamide gel, electrotransferred to a polyvinylidene fluoride membrane, blocked with 2% albumin for 1 h, and incubated with 1:1,000 dilution of a peptide-derived AQP4 polyclonal antibody raised in rabbits (7).

Light microscopy and immunocytochemistry. Tissues were fixed in situ by aortic perfusion with PBS containing 4% paraformaldehyde. Paraffin-embedded sections of brain, kidney, lung, trachea, spleen, liver, intestine, stomach, and skeletal muscle were stained with hematoxylin and eosin for examination by light microscopy. Sections were stained with the AQP4 antibody as described previously (7).

Water permeability in brain vesicles. Mouse brain fragments were homogenized by 20 strokes of glass Dounce homogenizer in PBS containing 250 mM sucrose, 10 mM Tris-HCl, pH 7.4, 1 μg/ml antipain, 1 μg/ml pepstatin, and 15 μg/ml benzamidine. The homogenate was centrifuged at 500 *g* for 10 min at 4°C, and adjusted to 1.4 M sucrose, 10 mM Tris-HCl, 0.2 mM EDTA (pH 7.4). A discontinuous sucrose gradient [2 M sucrose (3 ml), 1.6 M (6 ml), 1.4 M (12 ml, containing homogenate), 1.2 M (12 ml), 0.8 M (3 ml)] was centrifuged for 2.5 h at 25,000 rpm in an SW28 rotor, and 6-ml fractions were collected and assayed for total protein (Bradford) and AQP4 concentration. Osmotic water permeability (P_f) was measured in suspensions of membrane fractions (0.2–0.5 mg protein/ml) by the stopped-flow light-scattering method (22) using a 100-mM inwardly directed osmotic gradient. P_f was computed from the light-scattering signal and vesicle size (measured by quasielastic light scattering) as described previously.

Analysis of urinary concentration. Urine osmolalities of 35–40-d-old mice were measured before and after a 36-h water deprivation by the UCSF Clinical Chemistry Laboratory using freezing-point depression osmometry. To collect urine samples, mice were placed on a wire mesh platform in a clean glass beaker until spontaneous voiding was observed. The urine sample was collected immediately and kept on

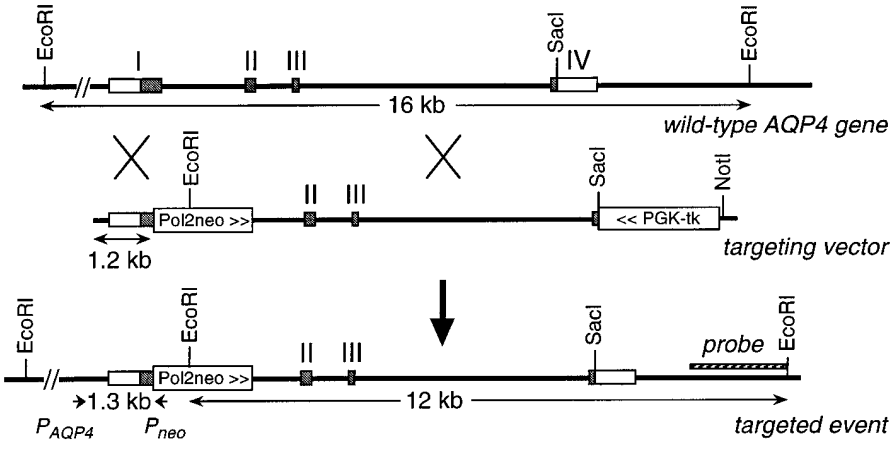

Figure 1. Targeting strategy for AQP4 gene interruption. The Roman numerals above the wild-type locus indicate AQP4 exons. Primers flanking the left arm were used for PCR screening of ES cell targeting. The probe (2.4 kb) was used for Southern blot analysis. The expected sizes of the EcoRI fragments that hybridize to the 2.4-kb probe (12 and 16 kb) are indicated.

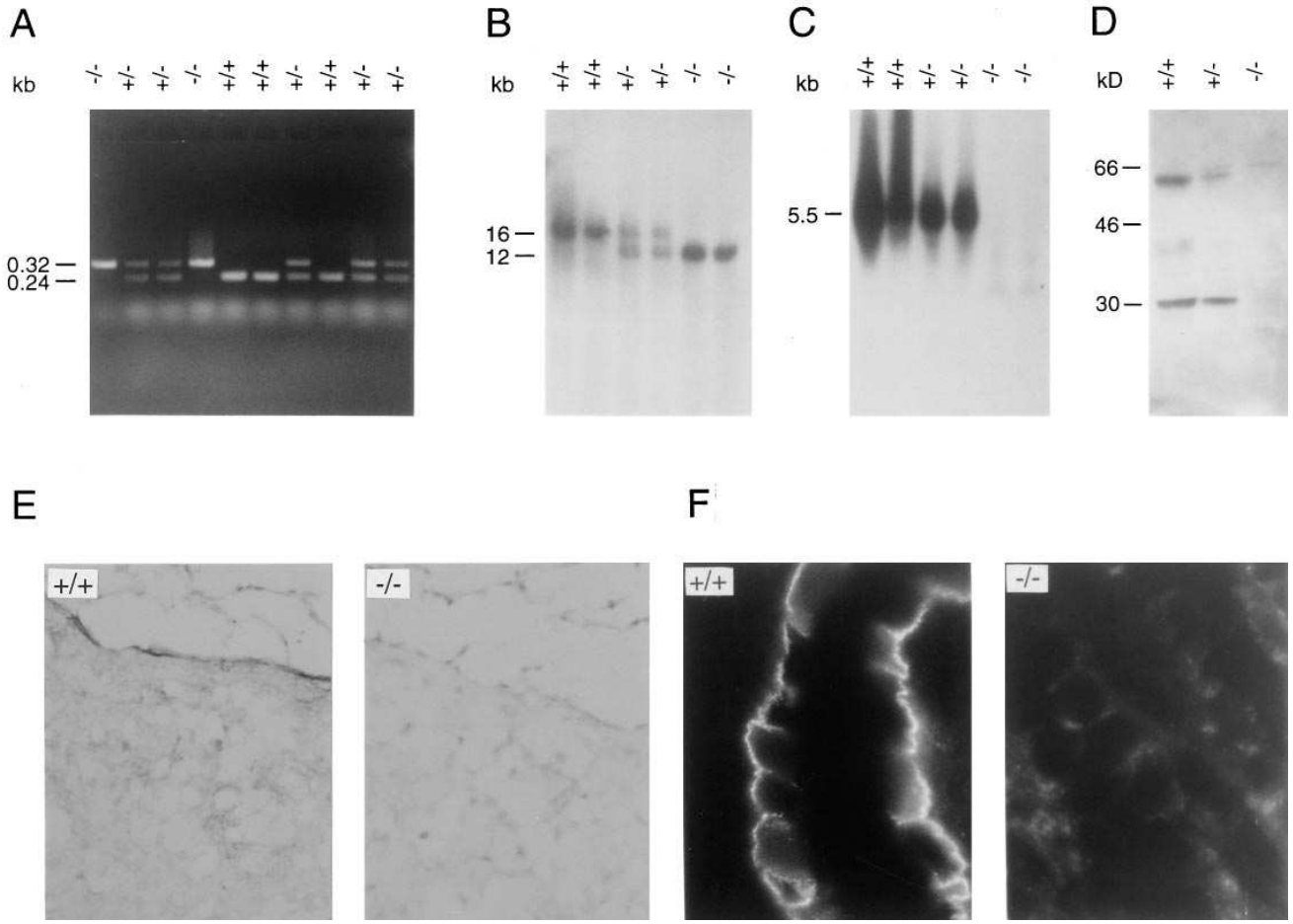

Figure 2. Analysis of AQP4 DNA, mRNA, and protein in transgenic mice. (*A*) PCR analysis of a litter from a single breeding showing wild-type [+/+], heterozygous [+/−], and homozygous AQP4 null [−/−] mice. (*B*) Southern blot of mouse liver genomic DNA digested with EcoRI and probed with a 2.4-kb genomic fragment (indicated in Fig. 1). (*C*) Northern blot probed with the mouse AQP4 coding sequence. (*D*) Immunoblot of brain membranes probed with AQP4 antibody. (*E*) Immunoperoxidase of AQP4 in the brain. (*F*) Immunofluorescence of AQP4 in the kidney medulla.

ice until osmometry. In some experiments, 0.4 μg/kg desmopressin was injected intraperitoneally after obtaining the 36-h urine sample, and a third urine sample was collected at 1–2 h after injection.

Neuromuscular evaluation. In addition to standard assessments of animal strength, coordination, and behavior, neuromuscular function was evaluated by performance on an accelerating rotorod (23, 24). According to protocol, mice were trained on the rod for 1 min at rest, 5 min at speed 1, and 1 min at rest. For testing, rod speed was incremented by 1 U every 2 min. Results were expressed as performance time on the rod before falling.

Results

Fig. 2 *A* shows a PCR genotype analysis of live mice born from a single mating of a heterozygote [+/−] pair. Wild-type [+/+], heterozygous [+/−], and homozygous [−/−] offspring were identified. Analysis of 164 live births (Table I) showed a genotype distribution that did not differ significantly from the Mendelian 1:2:1 ratio. Fig. 2 *B* shows a representative Southern blot confirmation of genotype. Northern blot analysis indicated strong expression of the full-length 5.5-kb AQP4 transcript in brain from [+/+] mice, with less expression of the 5.5-kb transcript in [+/−] mice, and minimal expression of only a truncated transcript in [−/−] mice (Fig. 2 *C*). Similar results were obtained with mRNA from the lung and kidney. The truncated AQP4 transcript is consistent with the site of gene interruption or may represent alternative splicing and polyadenylation.

Fig. 2 *D* shows no detectable AQP4 protein by immunoblot analysis of brain homogenates from [−/−] mice. There was a consistent reduction (by ~ 50%) in the amount of AQP4 protein in brain homogenates from [+/−] compared to [+/+] mice. Tissue immunocytochemistry from [+/+] mice revealed

Table I. Genotype Analysis of 164 Offspring from Intercross of AQP4 [+/−] Founders

	Genotype		
	+/+	+/−	−/−
Male	17	36	21
Female	24	47	19
Total	41	83	40

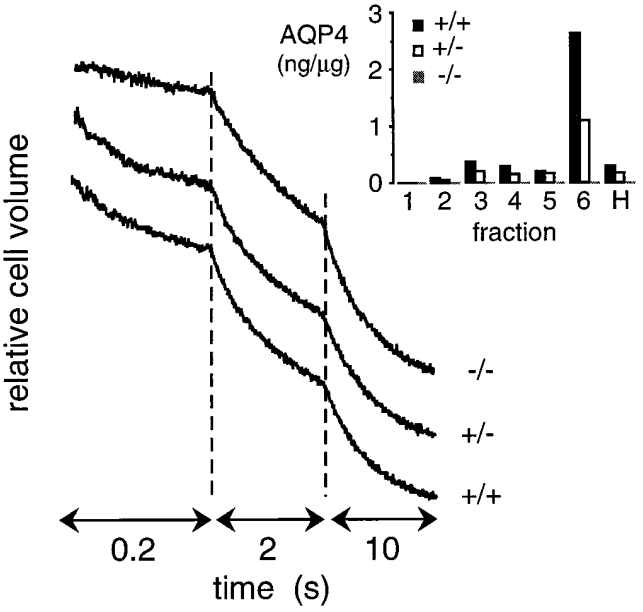

Figure 3. Functional analysis of AQP4 in the brain. Time course of light scattering in fractionated brain membrane vesicles subjected to a 100-mM inwardly directed sucrose gradient at 10°C. Data shown for fraction 6. (*Inset*) Specific expression of AQP4 protein (ng AQP4 protein/μg total protein) determined by quantitative immunoblot analysis.

the expected expression pattern of AQP4 in ependymal and astroglial cells in the brain (Fig. 2 *E*), and collecting duct basolateral membrane in the kidney (Fig. 2 *F*) (7). No detectable AQP4 protein was found in tissues from [−/−] mice.

Functional studies of water permeability were carried out in brain vesicles. Dissected cerebra were homogenized, nuclei and mitochondria were pelleted, and light microsomes were fractionated by sucrose density gradient centrifugation. Specific AQP4 expression in brain vesicle fractions from [+/+] mice was determined by quantitative immunoblot analysis and normalized to total protein (Fig. 3, *inset*). AQP4 protein expression was reduced by ~ 50% in [+/−] mice compared to [+/+] mice. Fraction 6 (~ 4% of total membrane protein) had the highest specific expression of AQP4 protein, and was analyzed functionally. No AQP1, AQP2, or AQP3 protein was detected in immunoblots of fraction 6 (not shown). Measurement of vesicle shrinkage in response to an osmotic gradient by stopped-flow light scattering (Fig. 3) indicated a subfraction of vesicles with high P_f (~ 0.04 cm/s at 10°C); P_f was not inhibited by 0.3 mM $HgCl_2$ (not shown). Highly water-permeable vesicles were not found in vesicle fractions isolated from the brains of [−/−] mice.

Analysis of growth by animal weight showed no differences among the genotypes (Fig. 4 *A*). Light microscopic examination of hematoxylin/eosin–stained sections of the brain, lung, kidney, trachea, stomach, and skeletal muscle showed no significant differences in morphology and structure in null vs. wild-type mice (not shown).

Urinary concentrating ability was evaluated from urine osmolalities after a 36-h water deprivation (Fig. 4 *B*). No significant differences in urine osmolalities were found in hydrated mice (just before water deprivation period). Serum sodium concentrations (range 151–161 mM) and osmolalities (range 304–335) also did not differ significantly among hydrated mice of [+/+], [+/−], and [−/−] genotypes ($n = 2$). However, there was a significant reduction in maximum urine osmolality in the [−/−] mice after a 36-h water deprivation ($P < 0.025$). Urine

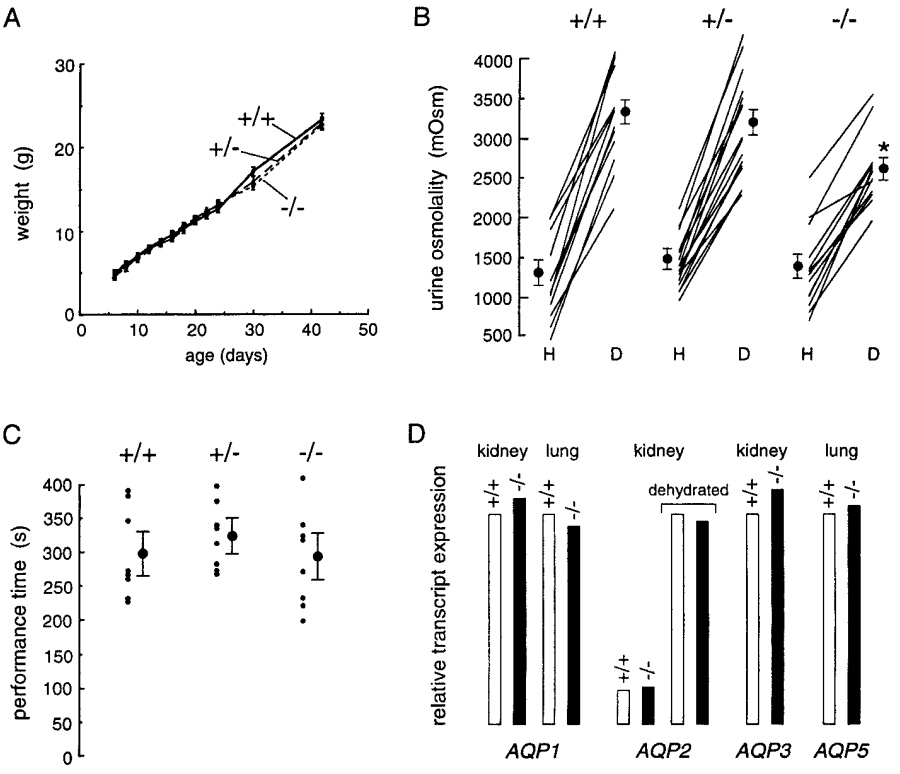

Figure 4. Phenotype analysis of transgenic mice. (*A*) Growth curve for 40 mice in each group. (*B*) Urine osmolalities before and after a 36-h water deprivation. *Significant difference with $P < 0.025$. (*C*) Rotorod neuromuscular evaluation shown as performance time before falling off of rod (see Methods). (*D*) Analysis of AQP transcript expression in wild-type vs. AQP4 null mice. Relative transcript expression was determined by quantitative densitometry of Northern blots (averaged data from two mice in each group) probed by ^{32}P-labeled coding sequences of indicated AQPs.

osmolalities in the 36-h–dehydrated mice did not increase further after desmopressin administration. These results demonstrate a mild urinary concentrating defect in the AQP4 null mice.

Neuromuscular evaluation was carried out by rotorod performance, which assesses composite neurological function, coordination, and skeletal muscle strength. After animal training according to established protocols, the times between placement on the rod and falling were measured. No significant differences were found ($P > 0.4$) (Fig. 4 *C*). Neurological evaluation by observation of behavior, and responses to sudden falling, tail lift, and similar maneuvers, showed no overt differences among the genotypes.

The hypothesis was tested that deletion of AQP4 is compensated for by upregulation of other AQPs. Northern blots of tissue mRNAs were probed with coding sequences of AQP1, AQP2, AQP3, and AQP5 (Fig. 4 *D*). As expected, dehydration produced a marked increase in AQP2 mRNA expression in the kidney. Transcript levels of the AQPs were not significantly different in the [−/−] vs. [+/+] mice. Immunoblot analysis of AQP1 protein in the kidney, brain, lung, and heart (not shown), and of AQP2 and AQP3 protein in the kidney (25) revealed no differences in expression. Immunostaining of the brain with antibodies against AQPs 1–3 also showed no differences in [+/+] and [−/−] mice (not shown).

Discussion

Transgenic null mice deficient in the AQP4 water channel were generated and characterized. The [−/−] knockout mice lacked detectable AQP4 protein. Analysis of 164 live offspring gave the predicted 1:2:1 ratio of [+/+]:[+/−]:[−/−] genotypes, indicating that there was no pre- or perinatal lethality. Animal growth and organ morphology were not affected by AQP4 deletion. These results suggest that AQP4 protein is not required for the development, survival, or growth of mice, and that phenotype abnormalities, if present, are subtle.

AQP4 is expressed with AQP3 at the basolateral membranes of principal cells in the kidney collecting duct (7), most strongly in the inner medulla (26). AQP4 water channels have thus been proposed to provide a pathway for water exit from principal cells into the hypertonic medullary interstitium. Principal cells also express the vasopressin-regulated water channel AQP2 in intracellular vesicles and at the apical plasma membranes. Defective maximum urinary concentration is predicted if AQP4 is responsible for the transport of a substantial quantity of water. The maximum urinary osmolality induced by water deprivation was decreased significantly in [−/−] mice compared to [+/−] and [+/+] mice. Recent measurements showed an ~ 4-fold decrease in vasopressin-stimulated water permeability in perfused segments of the inner medullary collecting duct in [−/−] vs. [+/+] mice (25). The absence of a more profound defect in urinary concentrating ability in the [−/−] mice is consistent with the notion that most of the water in the antidiuretic state is extracted osmotically by the cortical and outer medullary segments of the collecting duct. AQP3 may be the major basolateral membrane water channel in these segments.

AQP4 protein is most strongly expressed in astroglial cells in the brain and spinal cord, as well as in ependymal cells lining brain ventricles and in skeletal muscle plasmalemma. It was postulated that AQP4 deletion would cause serious neuromuscular abnormalities, including weakness, defective coordination, and neurological dysfunction. Interestingly, neuromuscular function was grossly normal, and quantitative rotorod performance analysis, which assays neuromuscular function and coordination (23, 24), showed no significant differences among the genotypes. The normal serum osmolality of [−/−] mice provides evidence against a role for AQP4 in osmosensing and osmoregulation. Further analysis will be required to identify possible subtle phenotypes (neuropsychiatric abnormalities, seizure threshold abnormalities), or neuromuscular defects that might develop in older mice.

AQP4 deletion was not associated with a change in the expression levels or patterns of the other mammalian AQPs. The AQP4 gene is located on human chromosome 18 (13), whereas the other aquaporin genes are on chromosomes 7, 9, and 12 (for review see references 27–29). The absence of a major phenotypic abnormality upon AQP4 deletion was an unexpected finding, and suggests that members of the AQP family (other than AQP2, reference 11) may not serve an essential physiological function. The absence of clinically overt abnormalities in AQP1-deficient humans (10) is consistent with this possibility. Phenotype analysis of multiple AQP knockout mice will be useful for further evaluation of AQP physiology.

Acknowledgments

We thank Dr. Walt Finkbeiner (University of California, San Francisco) for light microscopy analysis, Dr. Mark Knepper (National Institutes of Health) for advice in renal function studies, and Dr. Larry Tecott (Langley-Porter Psychiatric Institute) for help with the neuromuscular evaluation.

This work was supported by National Institutes of Health grants DK-35124, HL-42368, and HL-51854, and grant R613 from the National Cystic Fibrosis Foundation. The generation of mutant animals was supported by National Institutes of Health Gene Therapy Core Center DK-47766.

References

1. Zampighi, G.A., J.E. Hall, G.R. Ehring, and S.A. Simon. 1989. The structural organization and protein composition of lens fiber fractions. *J. Cell Biol.* 108:2255–2275.

2. Preston, G.M., and P. Agre. 1991. Isolation of the cDNA for erythrocyte integral membrane protein of 28 kilodaltons: member of an ancient channel family. *Proc. Natl. Acad. Sci. USA.* 88:11110–11114.

3. Fushimi, K., S. Uchida, Y. Hara, Y. Hirata, F. Marumo, and S. Sasaki. 1993. Cloning and expression of apical membrane water channel of rat kidney collecting tubule. *Nature (Lond.).* 361:549–552.

4. Ma, T., A. Frigeri, H. Hasegawa, and A.S. Verkman. 1994. Cloning of a water channel homolog expressed in brain meningeal cells and kidney collecting duct that functions as a stilbene-sensitive glycerol transporter. *J. Biol. Chem.* 269:21845–21849.

5. Ishibashi, K., S. Sasaki, K. Fushimi, S. Uchida, M. Kuwahara, H. Saito, T. Furukawa, K. Nakajima, Y. Yamaguchi, T. Gojobori, and F. Marumo. 1994. Molecular cloning and expression of a member of the aquaporin family with permeability to glycerol and urea in addition to water expressed at the basolateral membrane of kidney collecting duct cells. *Proc. Natl. Acad. Sci. USA.* 91: 6269–6273.

6. Echevarria, M., E.E. Windhager, S.S. Tate, and G. Frindt. 1994. Cloning and expression of AQP3, a water channel from the medullary collecting duct of rat kidney. *Proc. Natl. Acad. Sci. USA.* 91:10997–11001.

7. Frigeri, A., M. Gropper, C.W. Turck, and A.S. Verkman. 1995. Immunolocalization of the mercurial-insensitive water channel and glycerol intrinsic protein in epithelial cell plasma membranes. *Proc. Natl. Acad. Sci. USA.* 92: 4328–4331.

8. Hasegawa, H., T. Ma, W. Skach, M. Matthay, and A.S. Verkman. 1994. Molecular cloning of a mercurial-insensitive water channel expressed in selected water transporting tissues. *J. Biol. Chem.* 269:5497–5500.

9. Raina, S., G.M. Preston, W.B. Guggino, and P. Agre. 1995. Molecular cloning and characterization of an aquaporin cDNA from salivary, lacrimal, and respiratory tissues. *J. Biol. Chem.* 270:1908–1912.

10. Preston, G.M., B.L. Smith, M.L. Zeidel, J.J. Moulds, and P. Agre. 1994. Mutations in aquaporin-1 in phenotypically normal human without functional CHIP water channels. *Science (Wash. DC).* 265:1585–1587.

11. Deen, P.M., M.A. Verkijk, N.V. Knoers, B. Wieringa, L.A. Monnens, C.H. van Os, and B.A. van Oost. 1994. Requirement of human renal water channel aquaporin-2 for vasopressin-dependent concentration of urine. *Science (Wash. DC).* 264:92–95.

12. Jung, J.S., R.V. Bhat, G.M. Preston, W.B. Guggino, J.M. Baraban, and P. Agre. 1994. Molecular characterization of an aquaporin cDNA from brain: candidate osmoreceptor and regulation of water balance. *Proc. Natl. Acad. Sci. USA.* 91:13052–13056.

13. Yang, B., T. Ma, and A.S. Verkman. 1995. cDNA cloning, gene organization and chromosomal localization of a human mercurial-insensitive water channel: evidence for distinct transcriptional units. *J. Biol. Chem.* 270:22907–22913.

14. Ma, T., B. Yang, and A.S. Verkman. 1996. Gene structure, cDNA cloning and expression of a mouse mercurial-insensitive water channel. *Genomics.* 33:382–388.

15. Frigeri, A., M. Gropper, F. Umenishi, M. Kawashima, D. Brown, and A.S. Verkman. 1995. Localization of MIWC and GLIP water channel homologs in neuromuscular, epithelial and glandular tissues. *J. Cell Sci.* 108:2993–3002.

16. Shi, L.-B., and A.S. Verkman. 1996. Selected cysteine point mutations confer mercurial sensitivity to the mercurial-insensitive water channel MIWC. *Biochemistry.* 35:538–544.

17. Yang, B., and A.S. Verkman. 1997. Water and glycerol permeability of aquaporins 1-5 and MIP determined quantitatively by expression of epitope-tagged constructs in Xenopus oocytes. *J. Biol. Chem.* 272:16140–16146.

18. Yang, B., D. Brown, and A.S. Verkman. 1996. The mercurial-insensitive water channel (AQP-4) forms orthogonal arrays in stably transfected Chinese hamster ovary cells. *J. Biol. Chem.* 271:4577–4580.

19. Folkesson, H.G., M.A. Matthay, A. Frigeri, and A.S. Verkman. 1996. Transepithelial water permeability in microperfused distal airways. Evidence for channel-mediated water transport. *J. Clin. Invest.* 97:664–671.

20. Flamion, B., and K.R. Spring. 1990. Water permeability of apical and basolateral cell membranes of rat inner medullary collecting duct. *Am. J. Physiol.* 259:F986–F999.

21. Li, Y., T.T. Huang, E.J. Carlson, S. Melov, P.C. Ursell, J.L. Olson, L.J. Novel, M.P. Yoshimura, C. Berger, P.J. Chan, et al. 1995. Dilated cardiomyopathy and neonatal lethality in mutant mice lacking manganese superoxide dismutase. *Nat. Genet.* 11:376–381.

22. Van Hoek, A.N., and A.S. Verkman. 1992. Functional reconstitution of the isolated erythrocyte water channel CHIP28. *J. Biol. Chem.* 267:18267–18269.

23. Kuhn, P.L., E. Petroulakis, G.A. Zazanis, and R.D. McKinnon. 1995. Motor function analysis of myelin mutant mice using a rotorod. *Int. J. Dev. Neurosci.* 13:715–722.

24. Lavvan, E.W., C.A. Lisciotto, D.A. Gapp, and D.A. Weldon. 1989. Development of rotorod performance in normal and congenitally hypothyroid mice. *Behav. Neurobiol.* 52:411–416.

25. Ma, T., C.-L. Chou, B. Yang, M. Knepper, and A.S. Verkman. 1997. Decreased concentrating ability and inner medullary collecting duct water permeability in transgenic mice lacking aquaporin-4. *J. Am. Soc. Nephrol.* (Abstr.). In press.

26. Terris, J., C.A. Ecelbarger, D. Marples, M.A. Knepper, and S. Nielsen. 1995. Distribution of aquaporin-4 water channel expression within rat kidney. *Am. J. Physiol.* 38:F775–F785.

27. Verkman, A.S., A.N. van Hoek, T. Ma, A. Frigeri, W.R. Skach, A. Mitra, B.K. Tamarappoo, and J. Farinas. 1996. Water transport across mammalian cell membranes. *Am. J. Physiol.* 270:C12–C30.

28. Agre, P., and S. Nielsen. 1995. The aquaporin family of water channels in kidney. *Kidney Int.* 24:1057–1068.

29. Ma, T., B. Yang, and A.S. Verkman. 1997. Closely spaced tandem arrangement of AQP2, AQP5 and AQP6 genes in a 27 kilobase segment at chromosome locus 12q13. *Genomics*. 43:387–389.